CHAPTER 136

A THREEDIMENSIONAL MODEL OF A HOMOGENEOUS ESTUARY

by

Jürgen S ü n d e r m a n n [1)]

Summary

Basing on HANSEN's hydrodynamical-numerical method a threedimensional model of wind and tidally generated processes in a homogeneous estuary is developed. The model includes an arbitrary depth distribution and the simulation of a boundary layer near the bottom. Some numerical examples demonstrate the applicability for practical purposes.

1. Introduction

Mathematical models of the dynamics in homogeneous estuaries, coastal waters and shallow seas are presently in a worldwide practical use. Commonly they are based on the vertically integrated hydrodynamical differential equations. Thus, the vertical structure of the circulation field is not considered. This procedure turned out to be sufficient for many purposes, so for the investigation of tidal processes or the global wind generated circulation.

On the other side, vertically averaged stream velocities are of little evidence in the case of those propagation and transport processes which are essentially vertically structured, e.g. the movement of solid material.

The left part of fig. 1 shows a stream profile corresponding to the empirical exponential law, the assumption of a constant horizontal velocity gives a rather good approximation.

---

1) Professor, Technical University, Hanover, W. Germany

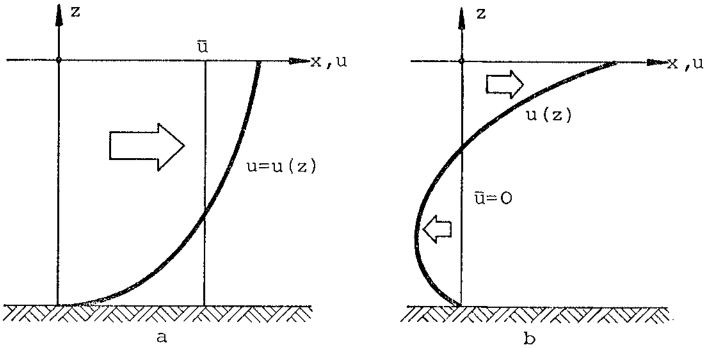

Fig. 1. Schematical vertical profiles of the stream velocity generated by tides (a) and by the wind stress (b)

Near the coastline, however, the real velocity distribution can deviate remarkably from a vertical mean. The right picture shows the typical vertical structure of a wind generated stream: the movement in the wind direction at the surface and a compensating countercurrent near the bottom. Although the mean velocity vanishes in this case, a considerable circulation occurs which may be connected with transport processes of dissolved constituents or sand. These processes can not be reproduced by the vertically integrated equations. Hence, its modelling requires the development of threedimensional models.

Vertically structured models are already used, especially in the field of physical oceanography, since several years (FRIEDRICH /1/). They have been developed, however for the baroclinic conditions of the deep ocean which are essentially different from the situation in coastal engineering.

Therefore, a specific threedimensional model has been developed (SÜNDERMANN /2/) which is presently being applied to the North Sea.

2. The model

The mathematical model is based on the following differential equations.

$$\frac{\partial u}{\partial t} + u\frac{\partial u}{\partial x} + v\frac{\partial u}{\partial y} + w\frac{\partial u}{\partial z} = -g\frac{\partial \zeta}{\partial x} + fv + \frac{\partial}{\partial z}\left(A_V\frac{\partial u}{\partial z}\right)$$

$$\frac{\partial v}{\partial t} + u\frac{\partial v}{\partial x} + v\frac{\partial v}{\partial y} + w\frac{\partial v}{\partial z} = -g\frac{\partial \zeta}{\partial y} - fu + \frac{\partial}{\partial z}\left(A_V\frac{\partial v}{\partial z}\right)$$

$$\frac{\partial \zeta}{\partial t} + u_s\frac{\partial \zeta}{\partial x} + v_s\frac{\partial \zeta}{\partial y} - w_s = 0$$

$$\frac{\partial u}{\partial x} + \frac{\partial v}{\partial y} + \frac{\partial w}{\partial z} = 0$$

ζ is the water level; u, v, w are the components of the velocity vector in a Cartesian system with coordinates x,y,z; f is the Coriolis parameter; g the earth's acceleration and A_V the vertical eddy coefficient. The index s refers to the surface.

The first two equations are obtained from the NAVIER-STOKES equation of motion with the assumption of a hydrostatic pressure distribution and the BOUSSINESQ approximation for the turbulent REYNOLDS stresses. The third equation is the formulation of the kinematic boundary condition at the surface. The last equation is the continuity equation for an incompressible medium.

In some cases, instead of the kinematic boundary condition, the vertically integrated continuity equation has been used. A horizontal turbulent exchange of momentum was introduced only if it was necessary for reasons of numerical stability and stationarity.

This system of hyperbolic partial differential equations is nonlinear and hence particularly suited to shallow water dynamics.

In addition, the following boundary conditions are added.

(a) $A_V \frac{\partial u}{\partial z}\Big|_s = \tau_s^{(x)}$, $A_V \frac{\partial v}{\partial z}\Big|_s = \tau_s^{(y)}$ at the surface, where $\tau_s^{(x)}$, $\tau_s^{(y)}$ are the components of the wind stress at the water surface.

(b) The normal component of the velocity vector vanishes at solid boundaries (coastline, bottom).

(c) The tangential component of the velocity vector vanishes at solid boundaries (non slip condition).

(d) Prescribed water elevations or stream velocities at the lateral open boundaries.

As initial condition a state of rest is assumed.

The discretization is carried out by means of a cubic grid net which is especially adapted to the structure of the basic differential equations, see fig. 2. It is related to the schemes of HANSEN /3/ and LEENDERTSE /4/.

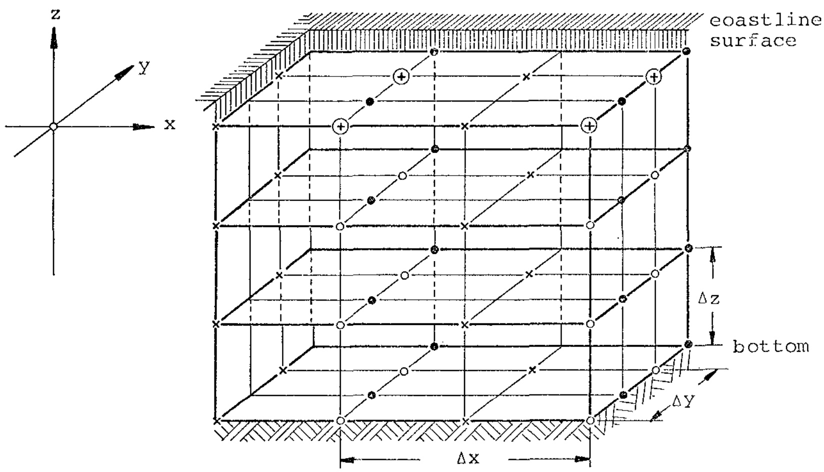

Fig. 2. Three dimensional computational grid. The unknowns are ealeulated in the following points

+ ζ × u • v o w ⊕ ζ and w

The horizontal space steps Δx and Δy are ehoosen equidistant. Indeed, this is not neeessary in prineiple, but it simplifieates the discretizised equations.

The vertieal grid distance Δz, however, should remain variable in any case, for an arbitrary refinement of the grid is impossible due to the enormously increasing eore memory demand. On the other hand, a relatively fine diseretization is required at interfaces (e.g. surface and bottom). For the same reason it is desirable to design the size of the grid elements near the surface or the bottom to be variable, in order to inelude the free moving surfaee and a variable depth distribution.

To fit the vertieal velocity profiles as observed in nature, it is neeessary to eonsider a boundary layer near the bottom. This ean be modeled by introdueing a coeffieient of vertieal eddy viscosity dependent on the depth. In the model presented here the relationship given by KAGAN /5/ has been used (fig. 3, upper pieture).

Analytical relationship (KAGAN 1968)

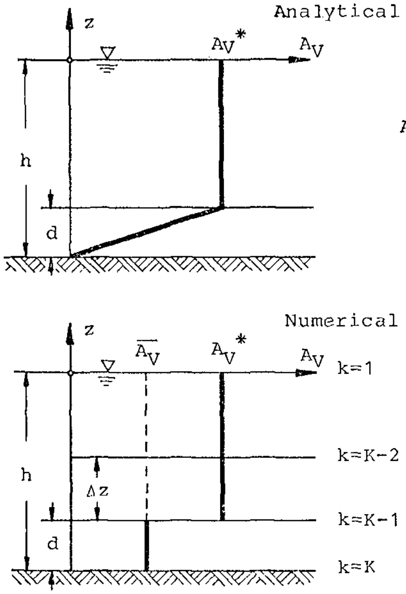

$$A_V(z) = \begin{cases} A_V^* \ , & \text{if } 0 \geqq z \geqq -h+d \\ \frac{z+h}{d} A_V^*, & \text{if } -h+d \geqq z \geqq -h \end{cases}$$

Numerical realization

$$u_{K-2} = (1+\kappa)\ u_{K-1}$$

$$\kappa = \frac{\overline{A_V}\ \Delta z}{A_V^*\ d}$$

Fig. 3. The dependence of the vertical eddy coefficient A_V on the water depth z

This relationship can be parametrizised by means of a dimensionless quantity κ with a value of 0,2 to 0,3 (fig. 3, lower picture).

Fig. 4. demonstrates that the best approximation of the empirical exponential profile will be reached for a value of κ = 0,3. For comparison, the profile is also drawn for a constant eddy coefficient (this assumption results in a more linear velocity profile).

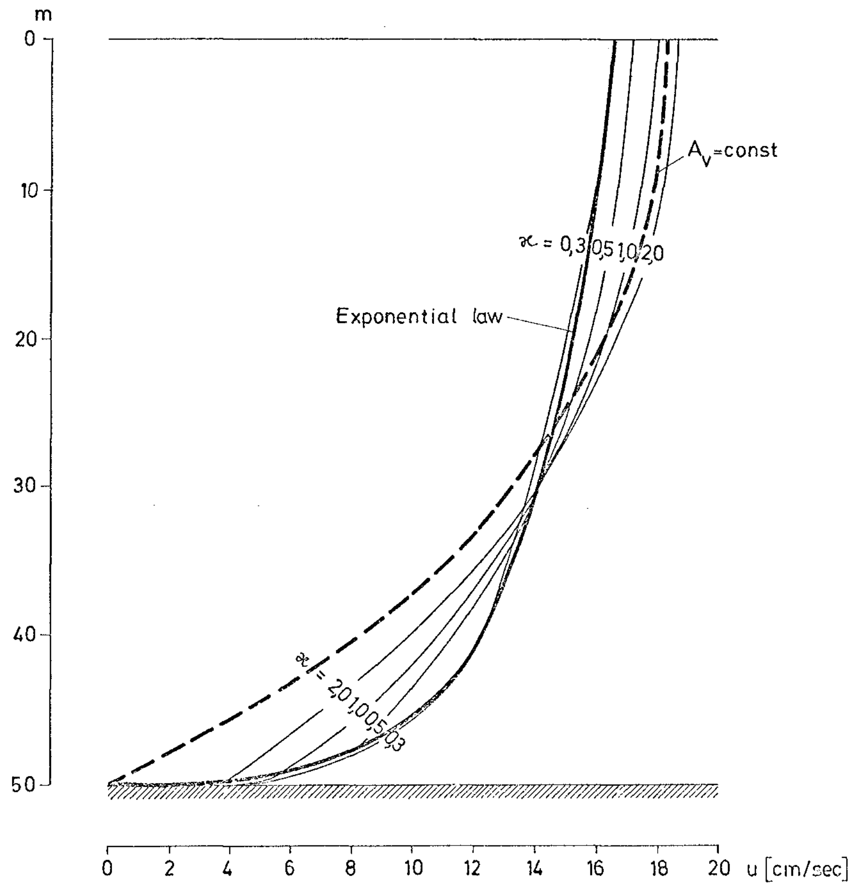

Fig. 4. Computed vertical profiles of tidal stream velocity for different models of the vertical eddy viscosity compared with the empirical exponential law.

The numerical solution of the differential equations is obtained by means of a finite difference method, firstly by using the explicit scheme of HANSEN for both, the horizontal and the vertical direction. As it turns out, the restrictions for numerical stability are given not so much by the well-known criterium of COURANT - FRIEDRICHS - LEWY:

$$\Delta t \leqq \frac{\Delta x}{\sqrt{gh}} ,$$

but by an additional condition for the vertical grid distance:

$$\Delta^2 z \leqq 2A_V \Delta t.$$

For instance, with $A_V = 0{,}1\ m^2\ sec^{-1}$ and $\Delta t = 300$ sec the vertical grid distance should be choosen as

$$\Delta z \geqq 7{,}75\ m.$$

Such a large grid cannot be accepted when investigating boundary layer phenomena.

In order to overcome this difficulty the well-known implicit procedure of CRANK - NICOLSON has been used for approximating the vertical diffusive term. This procedure allows one to choose the vertical grid distance Δz arbitrary. The technique also acts to stabilize the numerical computation to such an extent that the COURANT-criterium can be slightly extended.

If, for a given spatial discretization, the COURANT-criterium leads to an unsuitable computational effort, the equations of motion must also be solved by an implicit procedure for the horizontal direction. This can be achieved by type of alternating direction method combining the equations of motion and the vertically integrated continuity equation.

3. Some results for schematic models

The presented model is applied, firstly, to tidal and wind induced threedimensional circulation processes in schematic canals and basins. The following examples are based on a canal of constant depth (50 m) and a length of about 100 km or on a basin with 100 km length, 50 km width and 50 m depth. The models have an open boundary in the case of an incoming tidal wave (100 cm amplitude),they are closed in the case of wind generated motions

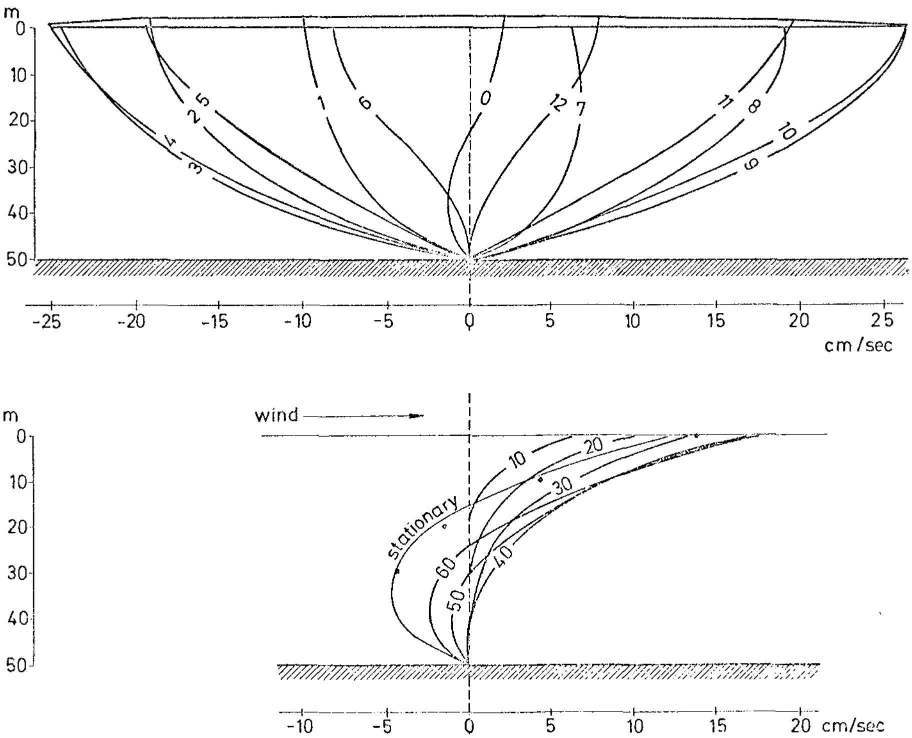

Fig. 5. Computed vertical velocity profiles in a canal of constant depth.

Upper picture: Tidal generated motion. The numbers are hours.

Lower picture: Wind generated motion. The numbers are minutes after the beginning of the wind.

(20 m/sec wind speed). Further values are:

$$A_V = 0{,}1 \text{ m}^2 \text{ sec}^{-1} \text{ and } f = 1{,}2 \cdot 10^{-4} \text{ sec}^{-1}$$

Fig. 5 shows some typical vertical velocity profiles for a point situated in the middle of a 50 m deep canal. In the upper picture the tidal flow for different tidal phases (in hours) has been drawn. It may be clearly seen that the alternation of the stream direction within the tidal cycle begins firstly in the deeper layer. The maximum velocities occur, generally, at the surface.

The lower picture shows the time dependent development of the velocity distribution under a stationary wind. The numbers are in minutes after the beginning of the wind's action. The counter-current near the bottom is formed after only 40 minutes. The points mark the analytical solution for the stationary linear case.

Fig. 6 shows, for the above considered example, the stationary circulation system along a longitudinal section. The upper figure demonstrates the corresponding water elevation.

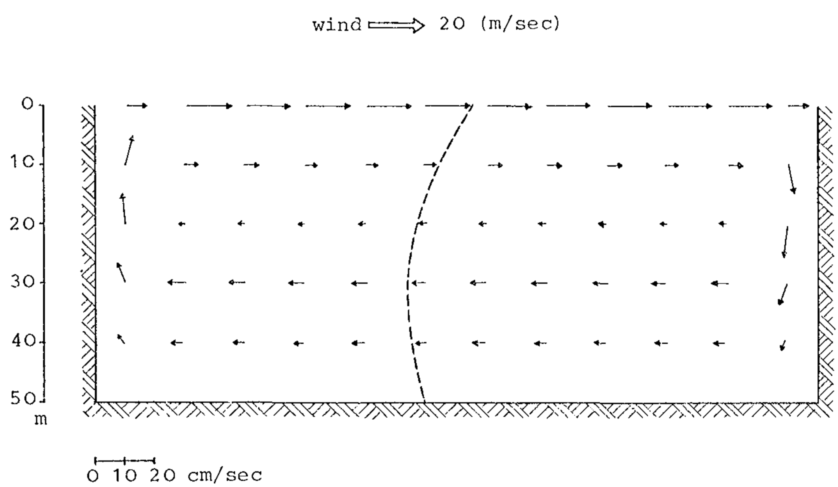

Fig. 6. Wind generated circulation field in a closed channel of constant depth. The dashed curve shows a vertical stream profile.

In fig. 7 the stationary stream fields are drawn for a constant Northerly wind at different depths, namely at the surface and for 10, 20, 30, 40, 50 m water depth. It is assumed, in this case, that even at the bottom a nonvanishing velocity can appear which generates an energy dissipation according to a quadratic friction law. One can clearly see a reduction and turning to the right, of the velocity vector with increasing depth.

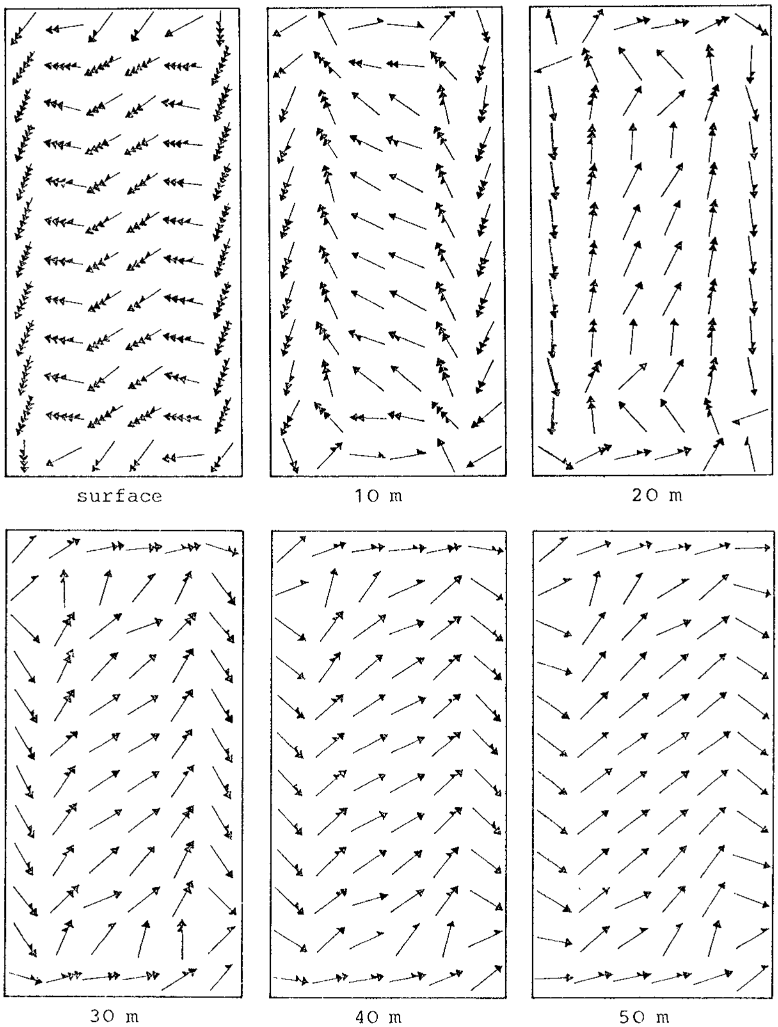

Fig. 7. Wind generated horizontal circulation field in a closed basin of constant depth for 6 horizons.

This fact suggests a comparison with the EKMAN theory of wind driven currents. Fig. 8 shows the velocity vectors for different depths for a point in the middle of the basin. The enveloping curve of the arrows should agree, in the ideal case, with the well-known EKMAN spiral (see the small sketch in the lower right corner). The theoretical EKMAN frictional depth

$$D = \pi\sqrt{\frac{2A_v}{f}} \simeq 40{,}7 \text{ m}$$

is in a good agreement with the computed value in the inner basin.

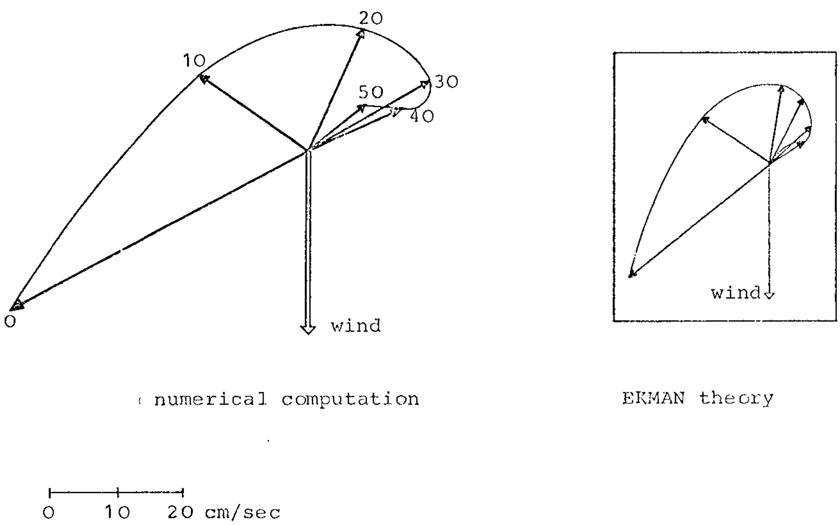

Fig. 8. The EKMAN spiral of the velocity vector for a Northerly wind over a basin of constant depth (the numbers are depths in meters).

It may also be seen from the last picture that for this depth the direction of the current is just opposite to the surface stream (which is the definition of the frictional depth).

Fig. 9 demonstrates a comparison with the unstationary EKMAN theory. This theory states that the right-hand deviation of the surface vector (at the Northern hemisphere) converges to the 45° direction in the form of a CORNU spiral (see the sketch in the lower right corner). The numbers are hours after the beginning of the wind. The agreement of the both hodographs is remarkable.

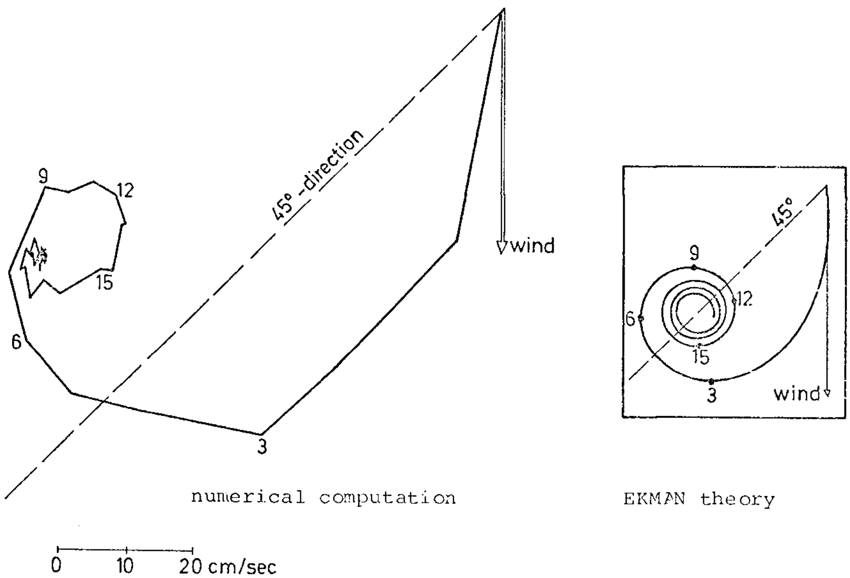

Fig. 9. The hodograph of the velocity vector at the surface for a Northerly wind over a basin of constant depth (the numbers are hours)

We shall deal now with tidal processes in schematic sea areas. Fig. 10 shows a longitudinal section with the tidal generated stream field in a canal for two tidal phases separated by a half tidal period. The tides are controled by the boundary conditions at the right boundary.

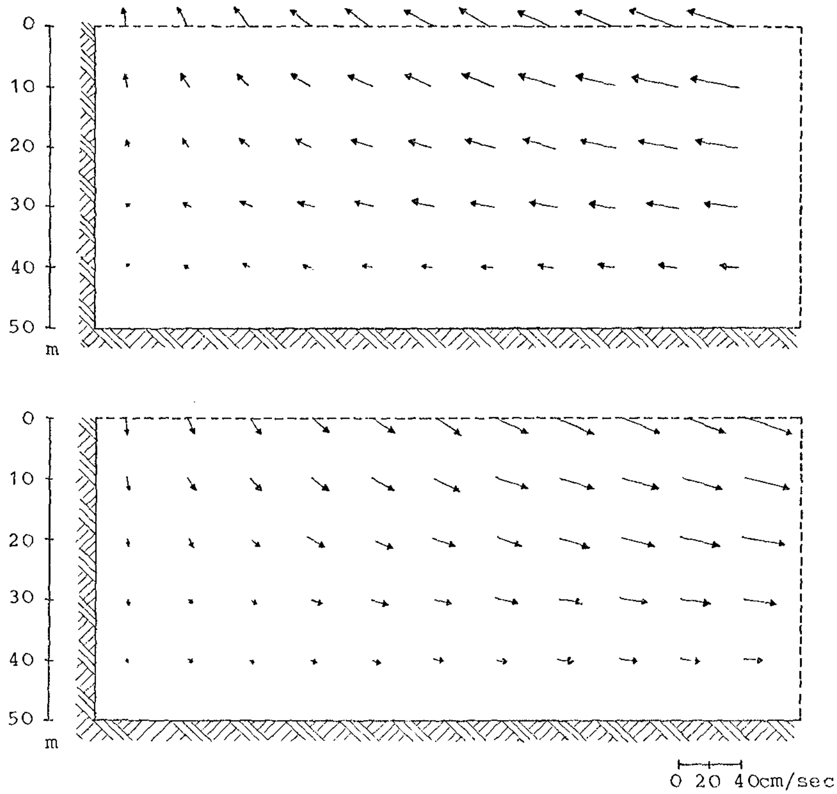

Fig. 10. Tide generated circulation field in an open channel of constant depth for two different phases.

It can be seen from the fig. 11 that also in the case of a variable depth distribution - here with a simple submarine barrier - reasonable velocity distributions are calculated.

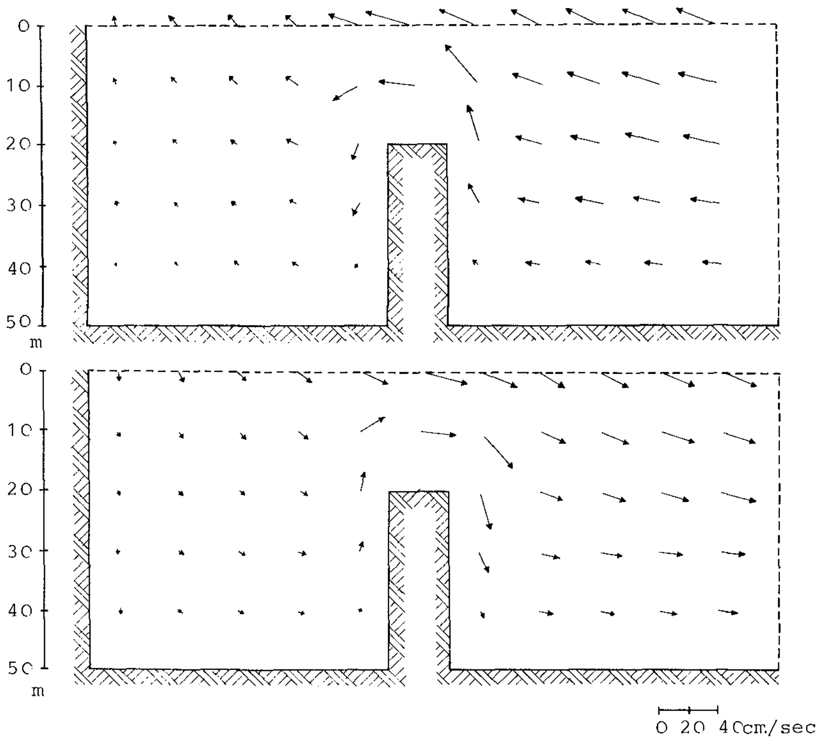

Fig. 11. Tide generated circulation field in an open channel with a submarine barrier for two different phases.

Summarizing it can be stated that with the presented results concerning the dynamics of schematic threedimensional bays the developed numerical method has been suffieiently tested. The assumption of simple geometrieal forms seems to be meaningful and neeessary for the test stage of a new model. On the other hand, by the introduction of a variable depth distribution and of a boundary layer near the bottom the model elearly approximates more natural eonditions. A first applieation to a real sea basin is given for the following North Sea model.

4. The North Sea Model

The starting point for the discretization was a horizontal grid net with a grid distanee of 37 km as has been used for several years at the Institute for Oceanography of the University of Hamburg. This model has been extended, as shown above, to a threedimensional model by the addition of further 10 eomputational planes in the vertieal direetion. This grid planes are situated at the surfaee, at a depth of 3, 6, 10, 25, 50, 150, 220, 300 meters and at 3 and 1 m above the bottom and the bottom itself. This diseretization ineludes that for small depths (e.g. in the Southern part of the North Sea) eertain grid planes are absent.

The model which has been developed by P. SCHÄFER /6/ is presently in a testing stage. The next three pietures show some preliminary results eoncerning the main semidiurnal M_2-tide.

Fig. 12 gives the eomputed co-range and eo-tidal lines (in em and hours after the moon's transit at the Greenwich meridian, resp.). As a eomparison the known result of a vertieally integrated model is presented simultaneously. The differenees are, in general, quite small.

The tidal streams at the different depths, however, show partially a remarkable variation and hence deviation from the mean integrated value. In the area near the coast of the middle part of the British Isles even the phenomenum oecurs that the orientation of the stream figures is ehanged. That means that the velocity veetor at the deeper layers is rotating in the opposite sense of that one of the surface.

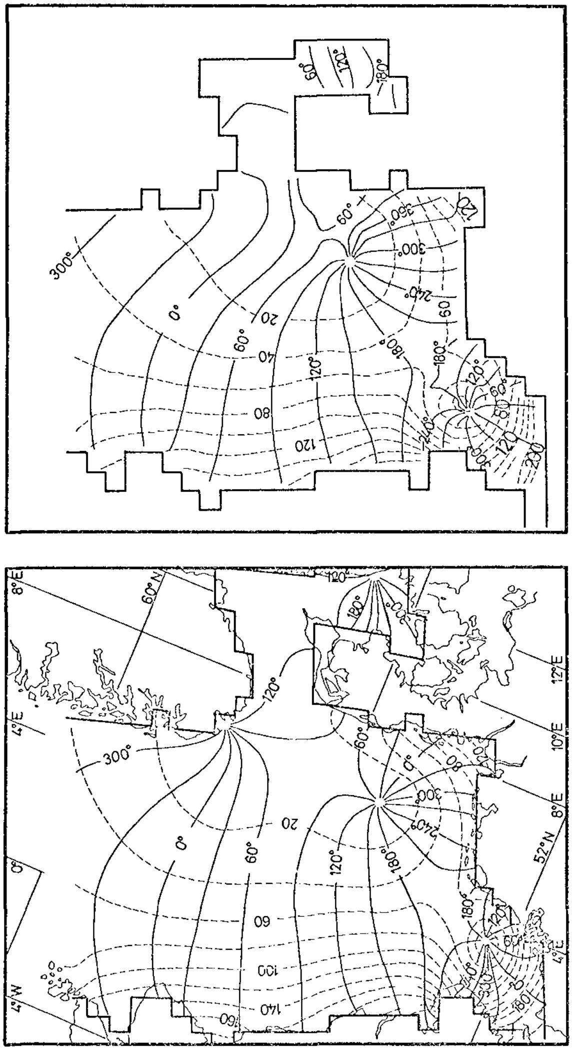

M_2-tide in the North Sea

ig. 12. Co-tidal lines related to Greenwich (———) and co-range lines in cm (-----) for a twodimensional (uper picture) and a threedimensional model with 11 layers (lower picture).

The figures 13 and 14, finally, demonstrate the computed stream figures for the depth horizons 10 m and 50 m of the Southern and Western part of the North Sea, resp.

Those numerical results may considerably extend our knowledge on the dynamics of this sea area. They open the possibility of a coupling with transport models describing the propagation of dissolved constituents and the movement of solid materials. It is intended to investigate the motion processes in real bays and estuaries in the same way. If this homogeneous models are tested sufficiently the distribution of salinity, temperature and density will be included in the model.

References

/1/ FRIEDRICH, H. Preliminary results from a numerical multi-layer model for the circulation in the North Atlantic, Deutsche Hydrographische Zeitschrift 23, 4, 1970

/2/ SÜNDERMANN, J. Die hydrodynamisch-numerische Berechnung der Vertikalstruktur von Bewegungsvorgängen in Kanälen und Becken, Mitt. Inst. Meereskd. Univ. Hamb. 19, 1971

/3/ HANSEN, W. Hydrodynamical methods applied to oceanographic problems, Mitt. Inst. Meereskd. Univ. Hamb. 1, 1962

/4/ LEENDERTSE, J.J. Aspects of the computational model for longperiod water wave progagation, RAND Memorandum 5294, Delft, 1967

/5/ KAGAN, B.A. Hydrodynamical models of ocean tides (in Russian), Gidrometeoroizdat, Leningrad, 1968

/6/ SCHÄFER, P. Ein dreidimensionales diagnostisches Nordseemodell zur Untersuchung großräumiger barokliner Bewegungsvorgänge, Doctor Thesis, University of Hamburg, 1974

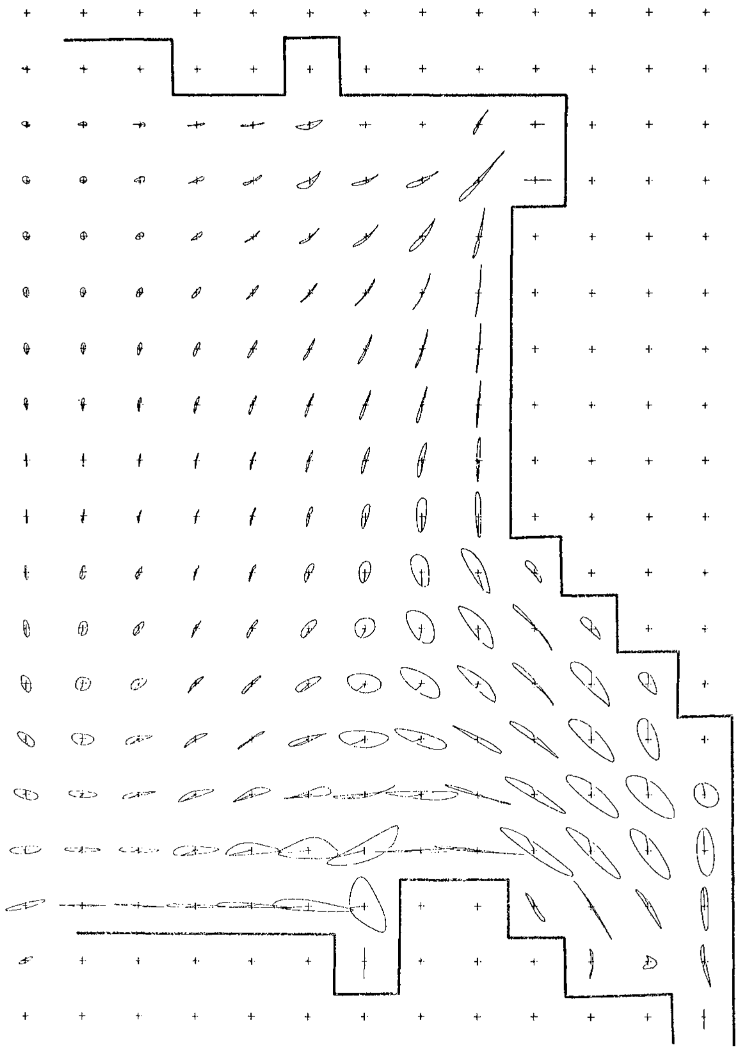

Fig. 13. M_2-tide in the North Sea.
Stream figures for 10m depth (Southern part)

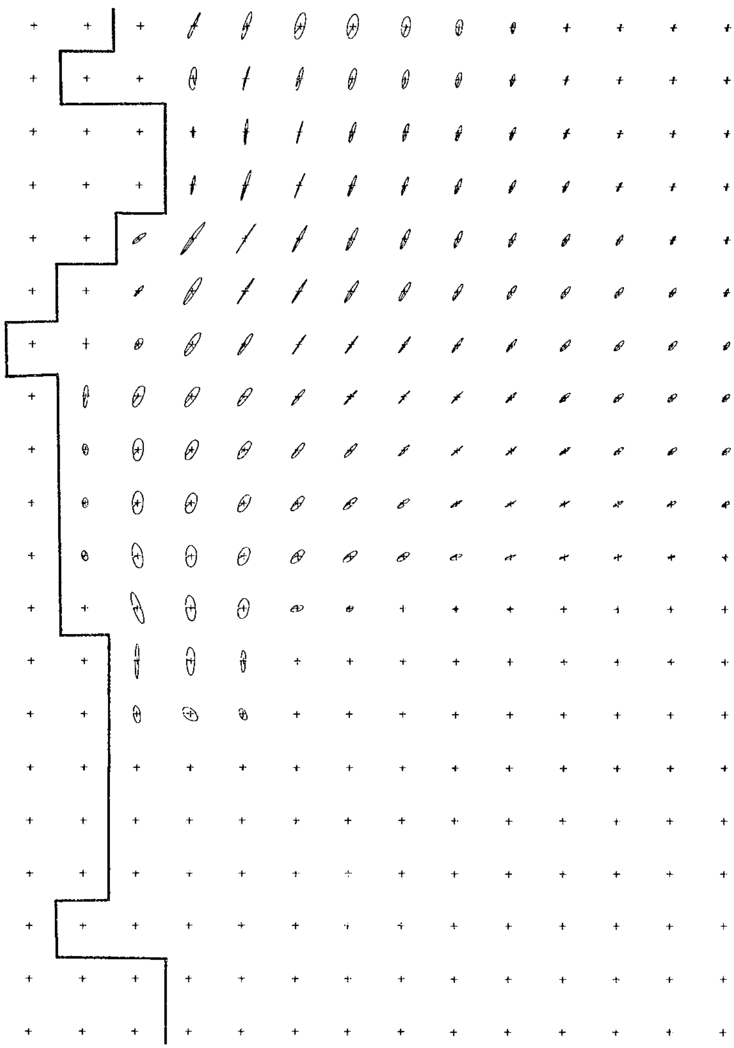

Fig. 14. M_2-tide in the North Sea.
Stream figures for 50 m depth (Western part)